Crack path for run-out specimens in fatigue tests: is it belonging to high- or very-high-cycle fatigue regime?

A. Shanyavskiy
State Center for Civil Aviation Flight Safety, Airport Sheremetievo-1, PO Box 54, Moscow region, Chimkinskiy State, 141426, Russia
shananta@mailfrom.ru

ABSTRACT. Fatigue tests run-out specimens up to 10^6 – $5x10^7$ load cycles are used to determine the stress level named "fatigue limit". Nevertheless, it is not clear what kind of fatigue cracking takes or will take place in these specimens. To discuss this problem, fatigue tests of titanium alloy VT3-1 specimens have been performed under tension with different values of R-ratio and under rotating-bending after various thermo-mechanical treatments (tempering, surface hardening and their combinations). Well-known S-N curves in High-Cycle-Fatigue regime have been plotted with run-out specimens usually used for "fatigue limit" determination. Then, after fatigue tests, run-out specimens have been tensed up to their failure, and fracture surface analyses have been performed for all tested specimens. It is found that run-out specimens in all combinations of treatments, for different R-ratio, have fracture surfaces for crack path in Very-High-Cycle-Fatigue regime. Based on this result, all S-N curves have been reconstructed in duplex curves for High- and Very-High-Cycle-Fatigue regime without using knowledge about "fatigue limit". Detailed fracture surfaces analyses have been developed, and crack paths have been compared for various combinations of materials and surface states.

KEYWORDS. Fatigue limit; Run-out specimens; Fractography; Subsurface crack path; Duplex S-N curves.

INTRODUCTION

Metals fatigue occurs in the Low- and High-Cycle-Fatigue (HCF) regime with crack origination on the surface. In the case of HCF, first of all sliding in different grains within the surface layer can be noted and, then, on the second stage after critical stress-state reached by the one of the sliding plane, volume rotation occurs that directs to free surface creation [1-3]. The same mechanism plays a dominant role in the Low-Cycle-Fatigue (LCF) regime, not only for crack origination. Metal in these two regimes has such a behavior as an opened synergetical system, and the surface layer accumulates most of all energy which goes in a metal volume during cyclic loading.

As is well-known, fatigue tests are performed up to stress level σ_{lim}, with many specimens have not failure at durability 10^7 – 10^8 load cycles, and this stress level (for not failed specimens, named "run-out") is named "fatigue limit".

Nevertheless, for lower stress levels and long lifetime (more than 10^8 load cycles), fatigue cracking exists for different materials, and area of crack origination appears at subsurface [4, 5]. Very-High-Cycle-Fatigue (VHCF) regime for metals has been discovered in tests with high frequency. Between VHCF and HCF regimes, a transition region exists, where fatigue crack origination on- and subsurface occurs with different probability under the same stress level. On the border of HCF area, probability of crack origination on the surface is approximately 100%, whereas probability of subsurface crack origination is equal to about zero.

Usually, dispersion of test results for constructing S-N curves in HCF regime is considered as material properties dispersion, with difference in a surface layer state from one to another specimen [1]. That is why "run-out" specimens are considered as S-N curve characteristic for HCF regime. But reality can be something different from that.
As far as "run-out" specimens are concerned, several possibilities exist in their cracking after interrupting fatigue tests: (1) crack origination takes place in specimens on the surface; (2) crack has not evidence on the surface but it exists in the subsurface; (3) crack is not on the specimen surface and not in the subsurface. In the third case, material behavior has to be considered as in VHCF regime with high probability.
The present paper discusses this problem related to titanium alloy Ti-6Al-4Mo (VT3-1), with different technological influence on the material state. The fractographic analysis for cracks path determination is essential in these investigations.

MATERIAL AND TESTING PROCEDURE

Tested specimens

Investigation has been performed on the two-phase titanium alloy Ti-6Al-4Mo (VT3-1) which is usually used in aircraft engines for manufacturing compressor disks and blades [6]. Metallographic investigations have shown that in specimen's material dominates mixed type (α+β) structure – lamellar plus globular.
The first group of specimens for tests was manufactured from two billets for compressor disks in their rim area. Smooth and notched bar specimens with stress concentration equal to about 1.46 were prepared in this case, Fig.1. The mechanical properties of the billets are shown in Table 1.

Disk № and standard	Ultimate tensile, σ_u, MPa	Elongation, δ %	Area reduction , Ψ %	Impact toughness, kgl/mm^2
I	1076	13.8	32.1	4.6
II	1083	13.4	27.1	3.3
Standard	≥ 960	≥9.0	≥20.0	≥ 3.0

Table 1. Mechanical properties of two titanium disks of VT3-1 alloy at 20°C.

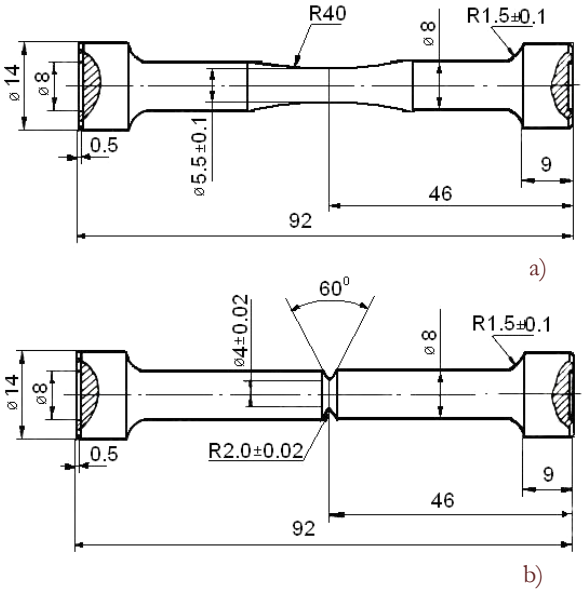

Figure 1. Schema of (a) smooth and (b) notched specimen, used in fatigue tests.

Some tested specimens (T) were tempered at 530°C during 6 hours and then cooled on the air. Some specimens were not tempered (NT). Some tempered specimens (TSP) were subjected to shot-peening procedure with metallic balls (0.05-0.3mm) up to intensiveness of residual stress 1.1-1.27. Some specimens were not tempered and not peened (NTP).

The second group of specimens was manufactured from a rod with mechanical properties shown in Table 2. The same type of specimens was manufactured from the rod for fatigue tests presented in Fig.1.

Specimen № and standard	Ultimate tensile, σ_u, MPa	Elongation, δ %	Area reduction, Ψ %	Impact toughness, kgl/mm^2
1	1048	14.0	14.5	4.1
2	1070	15.2	41.0	4.6
Mean value	1059	14.6	41.2	4.4
Standard	≥ 960	≥9.0	≥20.0	≥ 3.0

Table 2. Mechanical properties of the rod of titanium alloy VT3-1 at 20°C

Fatigue and tension tests

The first and the second group of specimens were tested with frequency 35 Hz and 200 Hz, respectively, at 20°C.
Two types of cyclic load tests were performed: rotating-bending and tension with different values of R-ratio and various maximum stress levels. After tests, fractographic analyses were performed on specimens subjected to different stress levels with durability in the range of $3x10^4$ - $3x10^7$ load cycles:
- notched bar NT- and NTP-specimens were fatigued under tension with R-ratio in the range of 0.3 to 0.76 , with maximum stress level in the range of 920 to 680 MPa;
- notched T- and TP-specimens experienced rotating-bending with maximum stress level in the range of 750 to 300 MPa;
- smooth T-specimens were tested in the range of R-ratio 0.41 to 0.64 , with maximum stress level in the range of 850 to 730 MPa;
- smooth TP-specimens experienced tension with R-ratio in the range of 0.3 to 0.67 , with maximum stress level in the range of 920 to 720 MPa.

T-specimens have not failed up to $5x10^7$ cycles under various positive R-ratios. Then, they were cyclically fatigued in the second stage of tests to their failure with higher stress amplitude, approximately in 2.3 time in accordance with previous stress level amplitude for R=-1.0.
All run-out specimens were subjected to monotonic tension on the "Instron" test-machine with low speed of grip.

Fractographic investigations

All fatigued and monotonically tensed specimens were subjected to fractographic analyses through the scanning electron microscope "EVO40" of the Karl Zeiss instruments. Fatigue striation spacings were measured to reproduce crack growth period and to evaluate the relationship between durability N_f and crack growth duration N_p.

RESULTS OF INVESTIGATION

Mono S-N curves

First of all, S-N curves were constructed for smooth T- and TP-specimens subjected to different tests condition (Fig.2). It is clear that, after tempering, durability of material decreases. This result reflects difference in surface state before and after tempering on the air. Surface layer has more intensive damage after tempering than before. The same result was found for steels [7].
Surface hardening of smooth specimens significantly influences durability, but this effect decreases with durability increasing. The discussed result was discovered for mean stress 600 MPa. Hardening effect can be negligible for long-life specimens because they reach durability area for transition zone from HCF to VHCF regime. In this case, a significant difference does not exist in durability for hardened and not hardened specimens of steels [8].
Notched specimens have not significant difference in regularities of their behavior under cyclic loads that were discussed related to smooth specimens (Fig.3). The T-specimens have a decrease in stress level (on 20-25%) for durability from 10^4 to $2x10^7$ load cycles.

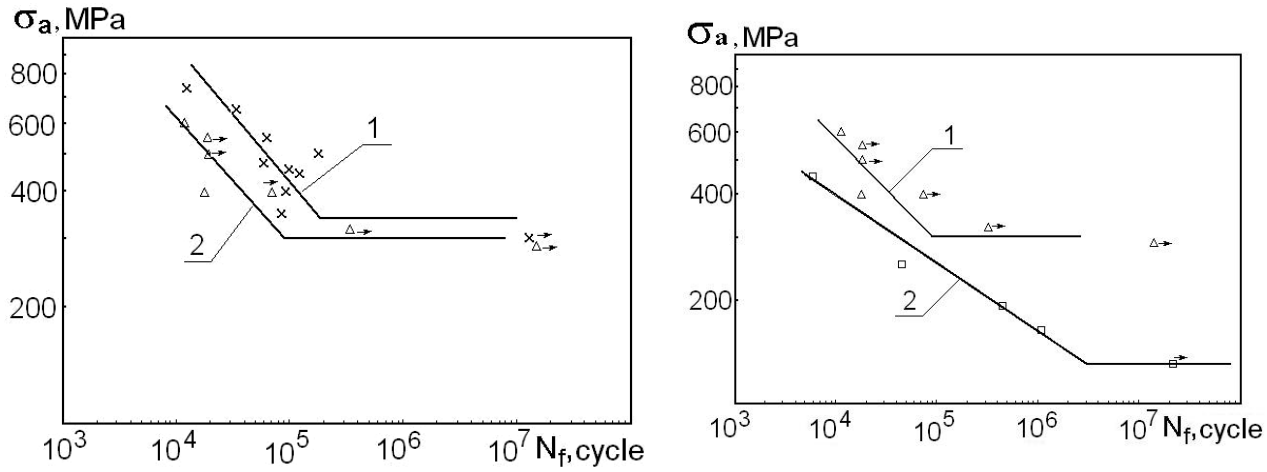

Figure 2: Mono S-N curves for tested smooth specimens: (a) symmetrical case for (1) not tempered and (2) tempered specimens; (b) at R>0 for (1) TP- specimens and (2) T-specimens.

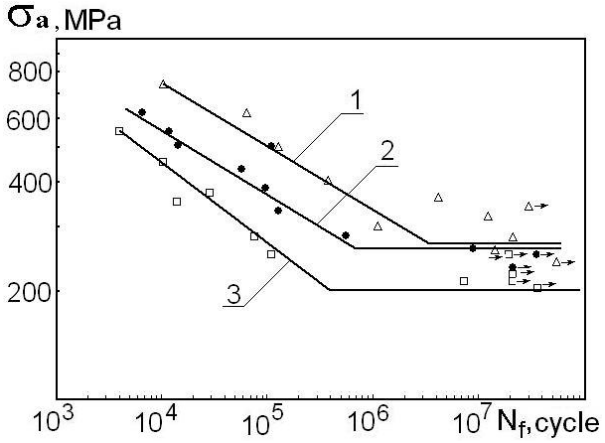

Figure 3: Mono S-N curves for notched (1) TP-specimens, (2) specimens without tempering and short peening, and (3) T-specimens tested under R=-1.0.

In all cases, fatigue tests were stopped in the range of durability (2-5)x10^7 cycles (see Fig.3). These not failed specimens were used for tensile test up to their failure to discover crack growth path from the fractographic analyses.

Crack path for failed specimens

Material behavior for hardened and not hardened specimens has significant difference in all range of stress levels. In hardened specimens, crack originates at the subsurface for durability being more than 5x10^5 load cycles, independent of the value of R-ratio. Number of origins has not a strong correlation with the maximum stress level. This fact can be explained on the basis of the maximum stress level value. This value was not far from the material Yield stress for high values of R-ratio. Nevertheless, in spite of high level of maximum stress (approximately 920 MPa) for R=0.67, the number of load cycles to failure can be reached (10^6 load cycles and more) that relayed to HCF regime.

In the case of low R-ratio in the range of 0.3-0.33, there were several origins in the fracture surface for maximum stress levels 920 and 900 MPa. For example, in the TP-specimen tested under maximum stress level 920 MPa, crack has not reached the specimen surface before fast fracture (Fig. 4). The first step of crack origination was realized because of smooth facet formation (the one by the α- phase).

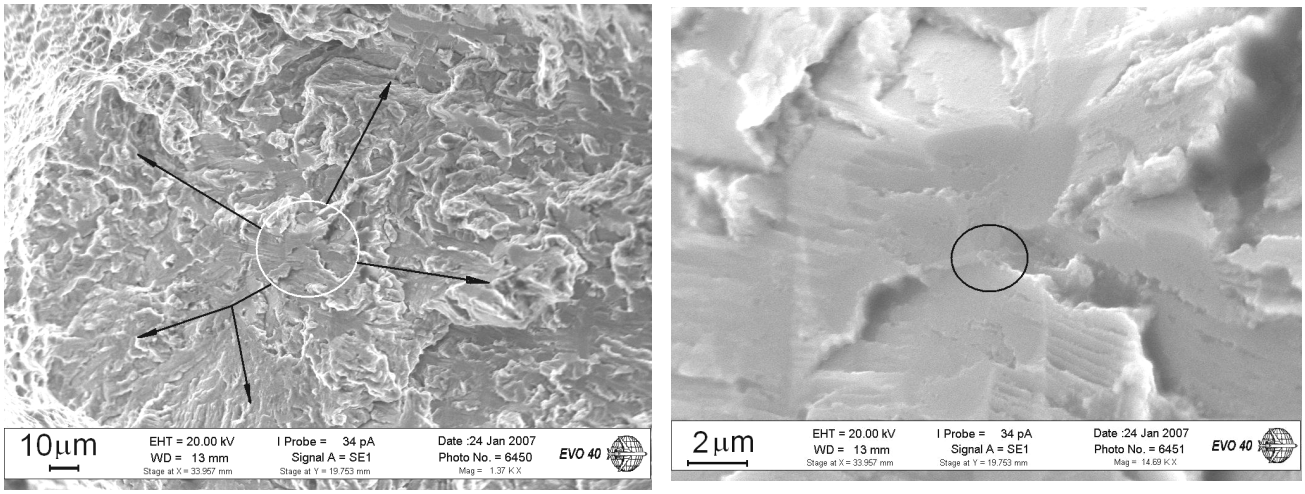

a) b)

Figure 4: (a) TP-specimen fracture surface with a subsurface origin; (b) presented under different magnification. Area of origin placed inside of the circle. Smooth facet in (b) is area of the first step of crack initiation by the α- phase.

Failed specimens under maximum stress level 900 MPa were cyclically loaded in the elastic-plastic regime, because this stress level is not far from material yield stress (see Tables 1, 2). Nevertheless, the area of origins in the fracture surface was in the subsurface as cleavage by the α- phase. It was the same as that found in HCF regime [9].

It was analysed the fracture surface pattern of the T - specimen subjected to maximum stress level 730 MPa with R=0.64 up to 2.3×10^7 load cycles without cracking. Then, this specimen was tested under maximum stress level 790 MPa with R=0.5 up to failure.

Fractographic analyses have shown that fracture origin is near the specimen surface (Fig.5a). This result shows that, under low stress level with bigger R-ratio, material has accumulation damages at subsurface, and fatigue crack could be appeared at subsurface for longer material stressing. This conclusion is based on earlier test results with two steps on stress levels of surface hardened and not hardened specimens of steels and Al-based alloy [10], [11].

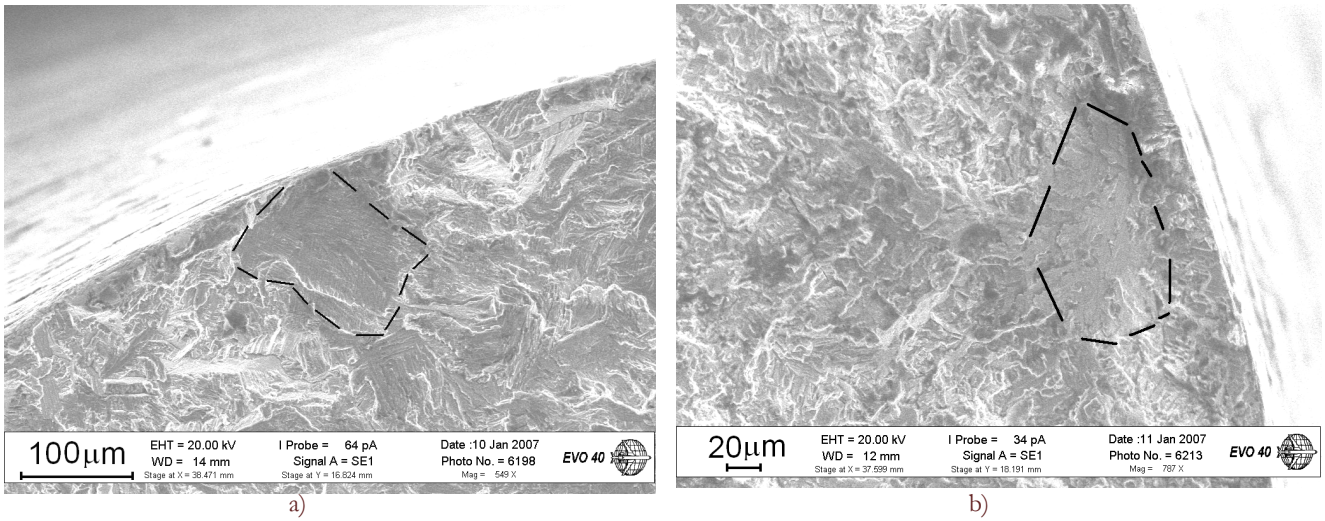

a) b)

Figure 5. Fracture subsurface origin (inside of the dashed line) (a) in the T - specimen tested, first, under maximum stress level 730 MPa with R=0.64 up to 2.3×10^7 load cycles without failure and, then, tested under 790 MPa with R=0.5 up to 4.1×10^5 cycles with failure, and (b) in NTP – specimen tested up to 1.8×10^6 load cycles with failure.

A similar result was found for NTP – specimen tested under maximum stress level 730 MPa with R=0.58. This specimen experienced 1.8 $\times 10^6$ load cycles before failure. Fracture surface pattern testified crack origination subsurface (see Fig.5b), with approximately the same surface formation.

Consequently, T – specimens in the range of 10^6 – 10^7 load cycles (and more) overaccumulated damages at subsurface very intensively. That is why crack origination can be at subsurface in spite of failed or not specimen for realized number of load cycles.
This conclusion has confirmation by results of investigations on fracture surfaces pattern tensed specimens that were not failed during cyclic tests in the range of 10^6 - 10^7 load cycles. Opened fracture surfaces under tension have shown that there exist subsurface brittle facets without evidence of dimples which surround these facets (Fig.6).

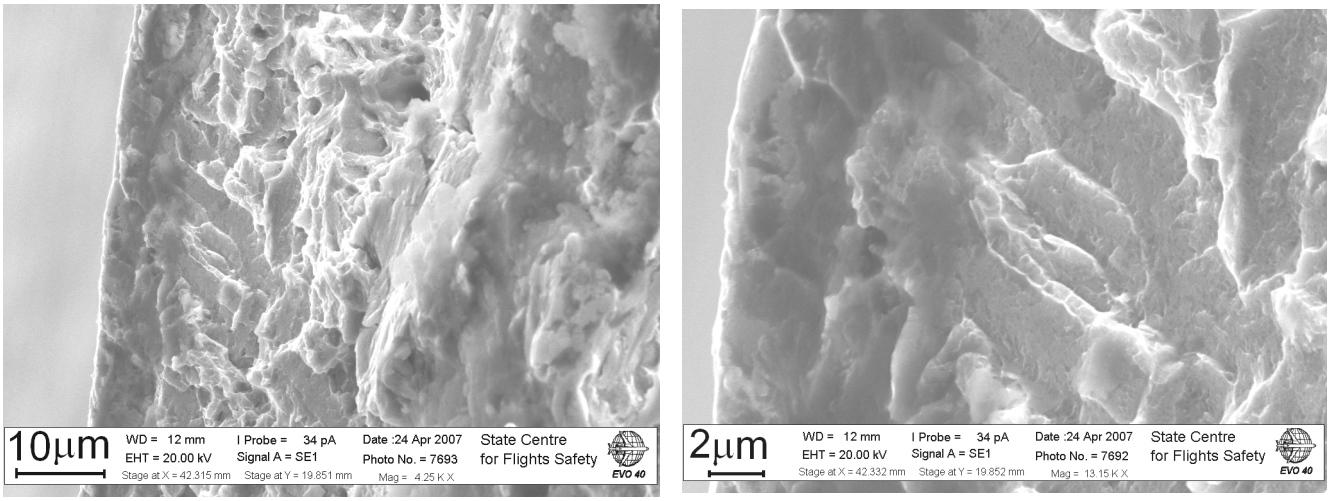

a) b)

Figure 6. Fracture subsurface pattern cyclically tested T- specimen up to 10^7 cycles without failure and, then, tensed up to failure.

Notched specimens have not shown the same significant clear tendency in subsurface crack origination as that found for smooth specimens. TS - specimens have shown subsurface crack origination in the range of (1.2 to 4.2)x10^6 load cycles. They were tested under negative R-ratio. That is why there are two factors, number of load cycles and negative R-ratio, that both influence subsurface crack origination. In the case of notched specimens, there is only one subsurface origin.

Discussion

The obtained fracture surface pattern for smooth specimens have been used to explain the tendency of the S-N curves at 10^6 load cycles, constructed for T- and TP – specimens (see Fig. 3). This tendency is related to difference in crack origination: crack origination for T- specimens is on the surface up to 10^6 load cycles, whereas crack origination is at subsurface for TP – specimens. In the case of number of load cycles more than 10^6, the probability of subsurface crack origination increases for T- specimens, and their number of subsurface cracking increases. Subsurface crack origination directs to decrease difference in durability for T- and TP – specimens. That is why using one S-N curve for approximation of all result of tested specimens can be seen to be the same S-N curve for T – and TP – specimens in the range of durability more than 10^6 load cycles.
The crack paths found for different cracked specimens of VT3-1 titanium alloy testified that tested specimens have to be selected for constructing bimodal durability distribution with two (or duplex) S-N curves – one for specimens with crack origination on the surface, and another one for specimens with crack origination subsurface. For several cases of studied specimens, duplex S-N curves are shown in Fig. 7.
Nevertheless, for usually constructed single S-N curves, tested specimens were selected in the range of durability 10^6 – 10^7 load cycles without failure. Then, their tensing and fracture surface investigation were employed to find the crack path and the place of crack origination.
Nevertheless, to construct S-N curves, tested specimens in the range of durability 10^6 – 10^7 cycles without failure should be selected. Then, their tensing and fracture surface investigation should be employed to find the crack path and the place of crack origination. In all fatigued specimens, there was measured fatigue striation spacing, and crack growth period was estimated for the stage of striations formation (Fig.8).

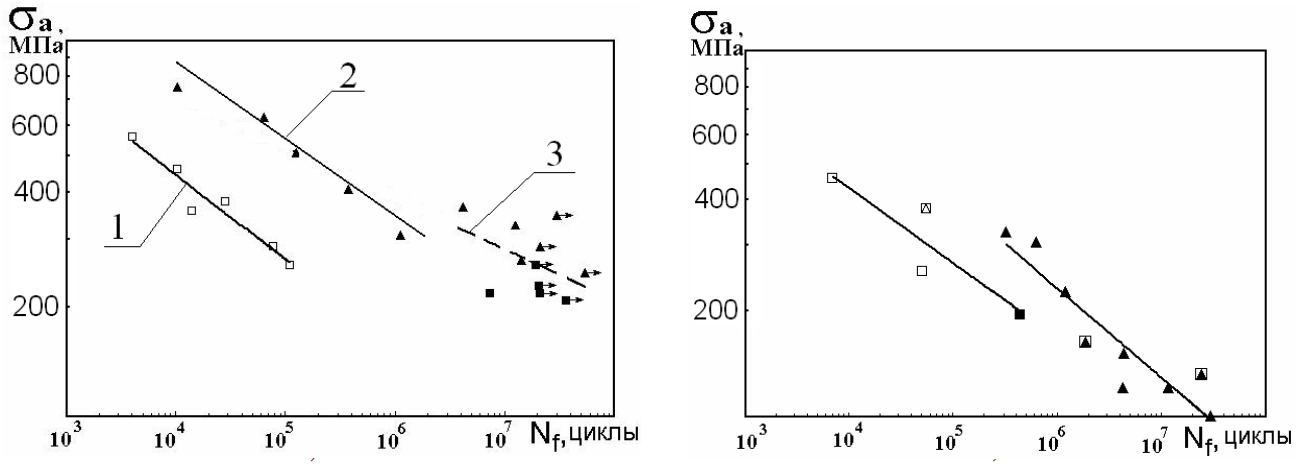

Figure 7. S-N curves: (a) for notched specimens subjected to stress ratio R=-1.0; (b) for smooth specimens at R=0.1. ▲ – TSP; □ – T; ■ – specimens failed under tension.

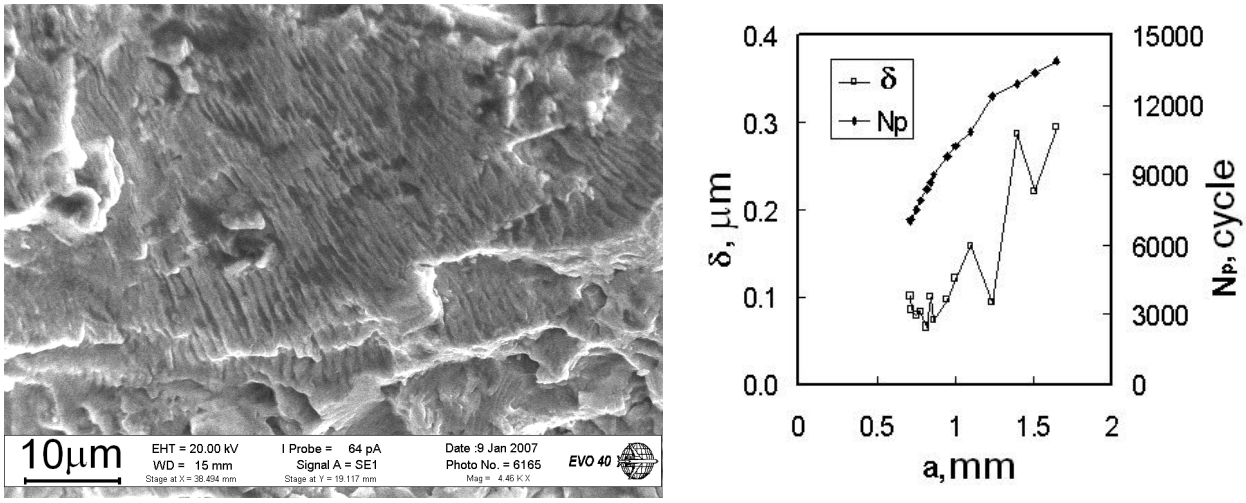

a) b)

Figure 8: View of : (a) fatigue striations in fracture surface of one of the fatigued specimens; (b) typical dependence fatigue striation spacing δ and number of load cycles Np on the crack length *a*.

Relationship N_p/N_f between crack growth period N_p and durability N_f has been estimated based on the above result, Fig.9. The evaluated dependence has the same tendency for all tested specimens without significant difference in the range of durability 10^6 – $2x10^7$ load cycles. TP – specimens have lower crack growth period for the same durability in accordance with the T – specimens. In notched specimens, crack growth period is more than that for smooth specimens at the same durability, but this difference has significance only for durability lower than $5x10^5$ load cycles. It can be summarized the above tendency by the following sequence: more crack growth period (on the stage of fatigue striation formation) for notched specimens without shoot peening; then lower growth period for notched and peened specimens; then smooth specimens without peening; and finally smooth-peened specimens.

Therefore, crack origination subsurface and on the surface with fatigue striations formation has approximately the same dependence relationship N_p/N_f against durability N_f. It can be used for aircraft structures to estimate durability by the results of fatigue striation spacing measurement or, based on knowledge about in-service durability, we have possibility to estimate crack growth period. This result agrees with earlier discovered possibility to estimate durability in low-cycle-fatigue for subsurface crack origination by the crack growth period based on the relation N_p/N_f against durability N_f , found for crack origination on the surface [12].

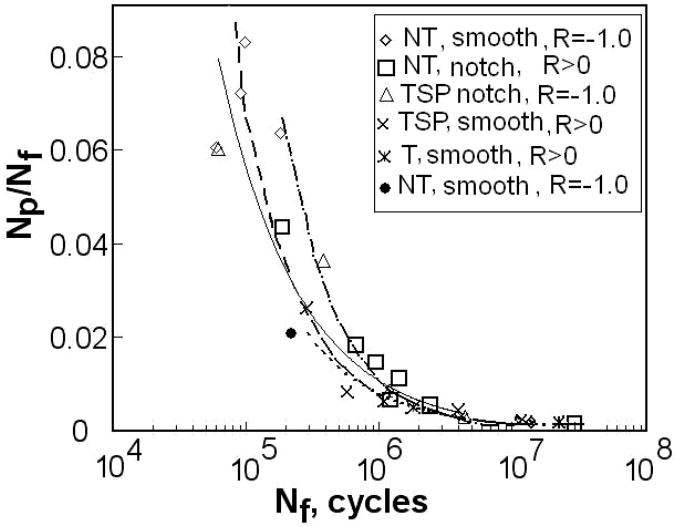

Figure 9. Ratio between crack growth period and durability N_p/N_f against durability N_f for the tested specimens after different termomechanical procedures

CONCLUSION

1. Test results of specimens manufactured from billets and rods of titanium alloy VT3-1 with two-phase ($\alpha+\beta$) globular and lamellar structure have shown that, in the range of cyclic stress near "fatigue limit", there exists transition from HCF regime to VHCF regime.
2. Crack path of "run-out specimens" not failed under cyclic tests and, then, tensed up to failure have fractographically been analysed. That has revealed fracture surface pattern related to VHCF regime with subsurface crack origination for different combination of tempering and surface hardening procedures.
3. Relationship between crack growth period and durability N_p/N_f against durability N_f for the tested specimens after different termomechanical procedures has the same tendency, and it can be used in practice to estimate the crack growth period in VHCF regime where fatigue striations have not evidence on the fracture surface.

REFERENCES

[1] Mughrabi ,H., Specific features and mechanisms of fatigue in the ultrahigh-cycle regime, Int. Journ. Fatigue, 28 (2006) 1501–1508.
[2] Panin, V.E., Panin A.V., Effect of surface layer in deformed solid body. Physical Mesomechanics, 8(5) (2005) 7-15.
[3] Shanyavskiy, A.A., Fatigue limit - Material property as an opened or closed system? Practical view on the aircraft components failures in GCF area. Int. J. Fatigue, 28(11) (2006) 1647 – 1657.
[4] Sakai, T., Ochi Y. (Eds) Very High Cycle Fatigue, Proc. Third Intern Conf VHCF-3, September 16-19, 2004, Ritsumeikan University, Kusatsu, Japan, (2004).
[5] Bathias, C., Paris, P.C., Gigacycle fatigue in mechanical practice, Marcel Dekker, NY, USA, (2005)
[6] Shanyavskiy, A.A., Losev, A.I., The effect of loading waveform and microstructure on the fatigue response of titanium aero-engine compressor disk alloys. Fatigue Fracture Engng Mater. Struct., 26 (2003) 329-342.
[7] Suh, C.-M., Hawing, B.W., Kim, S.C., Lee, T.S., A study on the fatigue characteristics of bearing steel in gigacycles. Proc. Third Intern Conf VHCF-3 (Sakai T. and Ochi Y. Eds), Ritsumeikan University, Kusatsu, Japan, (2004) 593-600.
[8] Liantao, L., Kazuaki, S., Effect of two-step load variation on gigacycle fatigue and internal crack growth behavior of high carbon-chromium bearing steel. Proc. Third Intern Conf VHCF-3 (Sakai T. and Ochi Y. - Eds), Ritsumeikan University, Kusatsu, Japan, (2004) 185-192.
[9] Shanyavskiy, A.A., Banov, M.D., The twisting mechanism of subsurface fatigue cracking in Ti–6Al–2Sn–4Zr–2Mo–0.1Si alloy, Engng Fracture Mechanics, 77 (2010) 1896–1906.

[10] Allison J.E., Jones J.W., Larsen J.M., and Ritchie R.O. (Eds) Fourth International Conference on Very High Cycle Fatigue, In.: Proc. Fourth Intern Conf VHCF-4, TMS, University of Michigan Ann Arbor, Michigan, USA, (2007).
[11] Shanyavskiy, A.A., Mechanisms of the 2024-T351 Al-Alloy Fatigue Cracking in Bifurcation Area after Laser Shocks Hardening Procedure, Key Engineering Materials, 465 (2011) 511-514.
[12] Shanyavskiy, A.A., The effect of loading waveform and microstructure on the fatigue response of Ti-Al-Mo alloys, Fatigue Fracture Engng Mater. Struct., 28 (2005) 195-204.